Hindawi
Journal of Chemistry
Volume 2021, Article ID 5547013, 8 pages
https://doi.org/10.1155/2021/5547013

Research Article

Isolation and *In Silico* Anti-COVID-19 Main Protease (M^{pro}) Activities of Flavonoids and a Sesquiterpene Lactone from *Artemisia sublessingiana*

Roza I. Jalmakhanbetova,[1] **Yerlan M. Suleimen**,[2] **Masayoshi Oyama**,[3] **Eslam B. Elkaeed**,[4] **Ibrahim. H. Eissa**,[5] **Raigul N. Suleimen**,[6] **Ahmed M. Metwaly**,[7] **and Margarita Yu. Ishmuratova**[8]

[1]*Kazakh University of Technology and Business, Nur-Sultan, Kazakhstan*
[2]*The Laboratory of Engineering Profile of NMR Spectroscopy, Sh. Ualikhanov Kokshetau University, Kokshetau, Kazakhstan*
[3]*Laboratory of Pharmacognosy, Gifu Pharmaceutical University, Gifu, Japan*
[4]*Department of Pharmaceutical Sciences, College of Pharmacy, AlMaarefa University, Ad Diriyah 13713, Riyadh, Saudi Arabia*
[5]*Pharmaceutical Medicinal Chemistry & Drug Design Department, Faculty of Pharmacy (Boys), Al-Azhar University, Cairo 11884, Egypt*
[6]*L.N. Gumilyov Eurasian National University, Nur-Sultan, Kazakhstan*
[7]*Pharmacognosy and Medicinal Plants Department, Faculty of Pharmacy (Boys), Al-Azhar University, Cairo, Egypt*
[8]*Department of Botany, E.A. Buketov Karaganda State University, Karaganda, Kazakhstan*

Correspondence should be addressed to Yerlan M. Suleimen; syerlan75@yandex.kz and Ahmed M. Metwaly; ametwaly@azhar.edu.eg

Received 5 February 2021; Accepted 8 May 2021; Published 27 May 2021

Academic Editor: Leena Gupta

The emergence of the COVID-19 pandemic declared the huge need of humanity for new and effective antiviral drugs. The reported antimicrobial activities of *Artemisia sublessingiana* encouraged us to investigate the ethanol extract of its aerial parts which led to the isolation of six flavonoids and a sesquiterpenoid. The structures of the isolated compounds were elucidated by EI-MS, 1D, and 2D NMR spectroscopic methods to be (1) eupatilin, (2) 3′,4′-dimethoxyluteolin, (3) 5,7,3′-trihydroxy-6,4′,5′-trimethoxyflavone, (4) hispidulin, (5) apigenin, (6) velutin, and (7) sesquiterpene lactone 8α,14-dihydroxy-11,13-dihydromelampolide. The isolated compounds were *in silico* examined against the COVID-19 main protease (M^{pro}) enzyme. Compounds 1–6 exhibited promising binding modes showing free energies ranging from −6.39 to −6.81 (kcal/mol). The best binding energy was for compound 2. The obtained results give hope of finding a treatment for the COVID-19 pandemic.

1. Introduction

COVID-19 is the pandemic caused by the new coronavirus strain SARS-CoV-2 (severe acute respiratory syndrome corona virus-2). The pandemic started in Wuhan, China, at the end of 2019 and spread all over the world [1]. By December 2020, COVID-19 infected more than 35 million patients and caused more than a million deaths according to the WHO [2]. Unfortunately, there is no accessible treatment for COVID-19 till now. The available treatment for infected patients is just symptomatic treatment by using anticoagulants, oxygen therapy, analgesics, and some research drugs [3]. Coronaviruses have caused serious diseases to humans before, such as Middle East respiratory syndrome (MERS-CoV) which appeared in 2012 and severe acute respiratory syndrome (SARS-CoV) in 2003 [4, 5].

The proteases, especially main protease (M^{pro}), play a vital role in the life cycle of coronaviruses [6]. M^{pro} is a cysteine protease that is enrolled in the maturation cleavage events within the polyprotein's precursors [7, 8]. This

enzyme is crucial for the processing and translation of polyproteins from the viral RNA [9]. Accordingly, M^{pro} is a very essential element for the replication and transcription of coronaviruses, and the inhibiting of its activity would block viral replication [10]. Consequently, M^{pro} could be an interesting target to explore the efficacy of new drugs against the coronavirus.

Now, there is an urgent need to find an effective drug against COVID-19. Since computational chemistry is a rapid and reliable screening method for bioactive compounds, there were many efforts to explore the effect of different ligands against COVID-19 [11–13].

Natural secondary metabolites are a significant source for anti-infective agents since dawn of history. These metabolites are found in many sources in nature such as plants [14, 15], marines [16, 17], and microbes [18–20], and they could be assorted following their chemical structure into countless classes such as saponins [21, 22], diterpenes [23], pyrones [24], isochromenes [25], flavonoids [26, 27], and alkaloids [28].

Artemisia L. (Asteraceae) species have been used in traditional medicine to treat various diseases and have shown several interesting pharmacological activities such as antimalarial, hepatoprotective, antioxidant, antibacterial, and cytotoxic activities [29–31]. Some flavonoids such as isorhamnetin-3-*O*-rutinoside and 5, 7, 4′-trihydroxy-6, 3′-dimethoxyflavone [32] have been isolated from *Artemisia sublessingiana* before. Furthermore, some sesquiterpene lactones like the eudesmanolide arsubin were also found in this species [33]. Secondary metabolites, such as flavonoids and sesquiterpenoids were reported to have diverse vital biological activities, such as antitumor [34], cytotoxic [35], antitrypanosomal [36], antibacterial, and anti-inflammatory activities [37].

In this study, the main bioactive contents of the aerial parts of *A. sublessingiana* (Krasch. ex Poljak.) Poljak. (Synonium *Seriphidium sublessingianum* (Krasch ex Poljakov)) have been investigated. This paper reports the isolation, structural determination, and *in silico* anti-COVID-19 main protease (M^{pro}) activities of six flavonoids and one sesquiterpene lactone from *A. sublessingiana*. Their structures were determined by spectrum analysis of 1D, 2D NMR, and ESI-MS data.

2. Materials and Methods

2.1. General Experimental Procedures. Column chromatography separations (CC) were performed on glass columns packed with silica gel (ASTM, 230–400 mesh, Merck, LTD, Japan). Thin-layer chromatography (analytical and preparative thin-layer chromatography (TLC) was performed on silica gel 60 F 254 glass plates (Merck, LTD, Japan). Spots were visualized under UV light (254 and 366 nm) and by spraying with alcoholic 10% H_2SO_4 reagent followed by heating. Isolated compounds were identified by 1D and 2D NMR analysis (^{1}H 500 MHz, ^{13}C 125 MHz), acquired on a Jeol Delta 2 NMR spectrometer at 297 K. Internal standards: TMS. Solvents: chloroform-*d*, acetone-d_6, and DMSO-d_6. Coupling constants are given in Hertz. The chemical shifts were expressed in δ ppm. Mass spectra (EIMS) were recorded on an IT-TOF-MS spectrometer.

2.2. Plant Material. The aerial parts of *A. sublessingiana* were collected 90 km from Kyzylorda city, Kazakhstan (Kyzylkum sand desert). The material was authenticated by Professor M. Ishmuratova, Department of Botany, E.A. Buketov Karaganda University, Republic of Kazakhstan. A sample was deposited in the herbarium of the Faculty of Biology and Geography.

2.3. Extraction and Isolation. Air-dried powered aboveground parts of *A. sublessingiana* (1.0 kg) were grounded and extracted with EtOH for 1 day. The extract was filtered, and the extraction process was repeated twice. The combined extracts were evaporated under reduced pressure to yield a crude extract of 93 g. The total crude extract was subjected to column chromatography over silica gel eluting with hexane and gradually increasing the polarity with acetone (up to 100%) and then MeOH. The fractions were studied on TLC and combined into twenty-three fractions (1F–23F). Compound (1) (216 mg) was separated from fraction 17F. Further chromatography of fraction 18F (2.5 g) on a column of silica gel with chloroform-acetone (in a manner of increasing polarity) and further chromatography of the obtained fractions 18F2 (0.1 g) with chloroform-methanol (in a manner of increasing polarity) gave compound (2) (5 mg). Fraction 18F4 (0.04 g) was dissolved in a solvent and repeatedly washed to give (3) (28 mg). Fraction 19F (2.91 g) was further fractionated on a silica gel column (60 g) eluting with chloroform-methanol (in a manner of increasing polarity) to obtain compounds (4) (19 mg) and (5) (15 mg). Fraction 14 F (0.65 g) was fractionated on a silica gel column eluting with chloroform-acetone (in a manner of increasing polarity) to give fraction (14F10). Fraction 14F10 (0.041 g) was further subjected to PTLC in system chloroform-methanol to obtain compound (6) (4 mg). Fraction 17F (2.93 g) was further purified by column chromatography on silica gel with chloroform-methanol (in a manner of increasing polarity) to give (7) (68.8 mg).

2.4. Compound Identification. 5,7-Dihydroxy-6,3′,4′-trimethoxyflavone (eupatilin) (1): yellow crystals, $C_{18}H_{16}O_7$. ^{1}H NMR (DMSO, 500 MHz) δ (ppm): 13.05 (s, 5-OH), 10.73 (s, 7-OH), 6.98 (s, H-3), 6.65 (s, H-8), 7.57 (d, $J = 2.5$ Hz, H-2′), 7.12 (d, $J = 8.5$ Hz, H-5′), 7.68 (dd, $J = 2.0$, 8.5 Hz, H-6′), 3.76 (s, 6-OCH_3), 3.88 (s, 3′-OCH_3), 3.86 (s, 4′-OCH_3); ^{1}H NMR ($CDCl_3$, 500 MHz) δ (ppm): 13.08 (s, 5-OH), 6.52 (s, 7-OH), 6.61 (s, H-3), 6.59 (s, H-8), 7.34 (brs, H-2′), 6.98 (d, $J = 8.5$ Hz, H-5′), 7.52 (brd, $J = 8.5$ Hz, H-6′), 4.05 (s, 6-OCH_3), 3.99 (s, 3′-OCH_3), 3.97 (s, 4′-OCH_3). ^{13}C NMR (DMSO, 500 MHz) δ (ppm): 163.38 (C-2), 103.37 (C-3), 182.21 (C-4), 152.74 (C-5), 131.35 (C-6), 157.32 (C-7), 94.38 (C-8), 152.43 (C-9), 104.13 (C-10), 122.92 (C-1′), 109.40 (C-2′), 149.00 (C-3′), 152.11 (C-4′), 111.67 (C-5′), 120.02 (C-6′), 59.97 (6-OCH_3), 55.73 (3′-OCH_3), 55.85 (4′-OCH_3).

HRESIMS: *m/z* 367.0780 $[M + Na]^+$, $C_{18}H_{16}O_7Na$, calc. 367.0788.

5,7-Dihydroxy-3′,4′-dimethoxyflavone(3′,4′-dimethoxyluteolin) (2): yellow amorphous powder, $C_{17}H_{14}O_6$. ^1H NMR (DMSO, 500 MHz) δ (ppm): 12.93 (s, 5-OH), 10.85 (s, 7-OH), 6.98 (s, H-3), 6.21 (d, $J = 2.5$ Hz, H-6), 6.54 (d, $J = 1.8$ Hz, H-8), 7.57 (d, $J = 1.8$ Hz, H-2′), 7.13 (d, $J = 8.6$ Hz, H-5′), 7.69 (dd, $J = 1.8$, 8.7 Hz, H-6′), 3.88 (s, 3′-OCH_3), 3.91 (s, 4′-OCH_3). HRESIMS: *m/z* 337.0686 $[M + Na]^+$, $C_{17}H_{14}O_6Na$, calc. 337.0683.

5,7,3′-Trihydroxy-6,4′,5′-trimethoxyflavone (3): yellow powder, $C_{18}H_{16}O_8$. ^1H NMR (DMSO, 500 MHz) δ (ppm): 12.99 (s, 5-OH), 10.70 (s, 7-OH), 9.60 (s, 3′-OH), 6.92 (s, H-3), 6.60 (s, H-8), 7.17 (dd, $J = 1.5$, 4.5 Hz, H-2′), 7.17 (dd, $J = 1.5$, 4.5 Hz, H-6′), 3.70 (s, 6-OCH_3), 3.70 (s, 4′-OCH_3), 3.80 (s, 5′-OCH_3). ^{13}C NMR (DMSO, 500 MHz) δ (ppm): 163.25 (C-2), 104.22 (C-3), 182.23 (C-4), 152.46 (C-5), 131.41 (C-6), 153.57 (C-7), 94.28 (C-8), 152.78 (C-9), 104.22 (C-10), 125.88 (C-1′), 102.12 (C-2′), 157.46 (C-3′), 139.63 (C-4′), 150.91 (C-5′), 107.68 (C-6′), 59.98 (6-OCH_3), 60.08 (4′-OCH_3), 56.15 (5′-OCH_3). HRESIMS: *m/z* 383.0740 $[M + Na]^+$, $C_{18}H_{16}O_8Na$, calc. 383.0737.

5,7,4′-Trihydroxy-6-methoxyflavone (hispidulin) (4): yellow powder, $C_{16}H_{12}O_6$. ^1H NMR (DMSO, 500 MHz) δ (ppm): 13.09 (s, 5-OH), 10.70 (brs, 7-OH), 10.40 (brs, 4′-OH), 6.79 (s, H-3), 6.60 (s, H-8), 7.93 (d, $J = 8.3$ Hz, H-2′), 6.93 (d, $J = 8.3$ Hz, H-3′), 6.93 (d, $J = 8.3$ Hz, H-5′), 7.93 (d, $J = 8.3$ Hz, H-6′), 3.74 (s, 6-OCH_3). ^{13}C NMR (DMSO, 500 MHz) δ (ppm): 163.80 (C-2), 152.40 (C-3), 182.14 (C-4), 152.78 (C-5), 131.34 (C-6), 157.26 (C-7), 94.23 (C-8), 152.40 (C-9), 104.07 (C-10), 121.21 (C-1′), 128.47 (C-2′), 115.96 (C-3′), 161.17 (C-4′), 115.96 (C-5′), 128.47 (C-6′), 59.95 (6-OCH_3).

5,7,4′-Trihydroxyflavone (apigenin) (5): yellow powder, $C_{15}H_{10}O_5$. ^1H NMR (DMSO, 500 MHz) δ (ppm): 12.98 (s, 5-OH), 6.79 (s, H-3), 6.20 (d, $J = 2.0$ Hz, H-6), 6.49 (d, $J = 2.5$ Hz, H-8), 7.94 (d, $J = 8.5$ Hz, H-2′), 6.93 (d, $J = 9.5$ Hz, H-3′), 6.93 (d, $J = 9.5$ Hz, H-5′),7.94 (d, $J = 8.5$ Hz, H-6′). ^{13}C NMR (DMSO, 500 MHz) δ (ppm): 163.23 (C-2), 103.34 (C-3), 182.28 (C-4), 161.96 (C-5), 99.35 (C-6), 164.65 (C-7), 94.48 (C-8), 157.82 (C-9), 104.20 (C-10), 121.68 (C-1′), 129.02 (C-2′), 116.46 (C-3′), 161.69 (C-4′), 116.46 (C-5′), 129.02 (C-6′).

5,4′-Dihydroxy-7,3′-dimethoxyflavone, luteolin 7,3′-dimethyl etherluteolin (velutin) (6): yellow powder, $C_{17}H_{14}O_6$. ^1H NMR ($CDCl_3$, 500 MHz) δ (ppm): 12.81 (s, 5-OH), 6.04 (brs, 4′-OH), 6.58 (s, H-3), 6.38 (d, $J = 2.0$ Hz, H-6), 6.50 (d, $J = 2.0$ Hz, H-8), 7.34 (d, $J = 2.0$ Hz, H-2′), 7.04 (d, $J = 8.3$ Hz, H-5′), 7.50 (dd, $J = 8.3$, 2.0 Hz, H-6′), 3.89 (s, 7-OCH_3), 4.01 (s, 3′-OCH_3).

8α,14-Dihydroxygermacra-1(10)E,4E-dien-6β,7α,11βH-12,6-olide (8α,14-dihydroxy-11,13-dihydromelampolide) (7): colorless crystals, $C_{15}H_{23}O_4$. ^1H NMR (CDCl, 500 MHz) δ (ppm): 5.49 (m, 2H, $J = 7.0$, 9.0, 16.0 Hz, H-1), 2.14 (m, H-2a), 1.89 (m, H-2b), 2.16 (m, H-3a), 1.91 (m, H-3b), 5.01 (brd, $J = 10.0$ Hz, H-5), 4.53 (t, $J = 10.0$ Hz, H-6), 2.12 (m, H-7), 3.90 (brs, H-8), 2.32 (brd, $J = 15.0$ Hz, H-9a), 2.25 (dd, $J = 3.0$, 15.0 Hz, H-9b), 2.57 (m, H-11), 1,43 (d, $J = 6.0$ Hz, H-13), 4.33 (brd, $J = 12.0$ Hz, H-14a), 4.13 (brd, $J = 12.0$ Hz, H-14b), 1.83 (brs, H-15), 2.84, 3.90 (brs, each, OH-3, 4). ^{13}C NMR (CDCl, 500 MHz) δ (ppm): 128.73 (C-1), 25.22 (C-2), 38.05 (C-3), 138.58 (C-4), 124.60 (C-5), 77.26 (C-6), 55.17 (C-7), 73.75 (C-8), 35.15 (C-9), 139.02 (C-10), 41.73 (C-11), 179.45 (C-12), 16.41 (C-13), 69.22 (C-14), 17.24 (C-15).

2.5. Docking Studies Experiment. The crystal structure of the target enzymes COVID-19 main protease (M^{pro}) (PDB ID: 6lu7, resolution: 2.16 Å) was downloaded from Protein Data Bank (http://www.pdb.org). Molecular operating environment (MOE) was used for the docking analysis [38]. In these studies, the free energies and binding modes of the examined molecules against M^{pro} were determined. At first, the water molecules were removed from the crystal structure of M^{pro}, retaining only one chain which is essential for binding. The cocrystallized ligand (PRD-002214) was used as a reference ligand. Then, the protein structure was protonated, and the hydrogen atoms were hidden. Next, the energy was minimized, and the binding pocket of the protein was defined [39].

The structures of the examined compounds and the cocrystallized ligand were drawn using ChemBioDraw Ultra 14.0 and saved in SDF format. Then, the saved file was opened using MOE software, and 3D structures were protonated. Next, the energy of the molecules was minimized. The validation process was performed for the target receptor by running the docking process for only the cocrystallized ligand. Low RMSD values between docked and crystal conformations indicate valid performance [40, 41]. The docking procedures were carried out utilizing a default protocol. In each case, 30 docked structures were generated using genetic algorithm searches. The output from MOE software was further analyzed and visualized using Discovery Studio 4.0 software [42, 43].

3. Results and Discussion

3.1. Compounds Isolation. Using different chromatographic techniques, seven compounds have been isolated from the ethanol extracts of the aerial parts of *A. sublessingiana*. The obtained compounds were identified using different 1D and 2D NMR spectroscopic methods to be (1) eupatilin [44, 45], (2) 3′,4′-dimethoxyluteolin [46–48], (3) 5, 7, 3′-trihydroxy-6,4′,5′-trimethoxyflavone [49], (4) hispidulin [50, 51], (5) apigenin [52, 53], (6) velutin [54], and (7) sesquiterpene lactone 8α,14-dihydroxy-11,13- dihydromelampolide [55–57]. The chemical structures of compounds (1–7) were confirmed by comparison of the reported spectral data in the literature (Figure 1).

3.2. Docking Studies. Docking studies were carried out for compounds (1–7) against the COVID-19 main protease (M^{pro}) (PDB ID: 6lu7, resolution: 2.16 Å) to examine the mode of binding with the proposed target. The cocrystallized ligand (PRD-002214) was used as a reference molecule. The results of docking studies revealed that the docked compounds have good binding affinities against COVID-19 main protease with binding free energies ranging from −4.94 to −6.81 kcal/mol (Table 1).

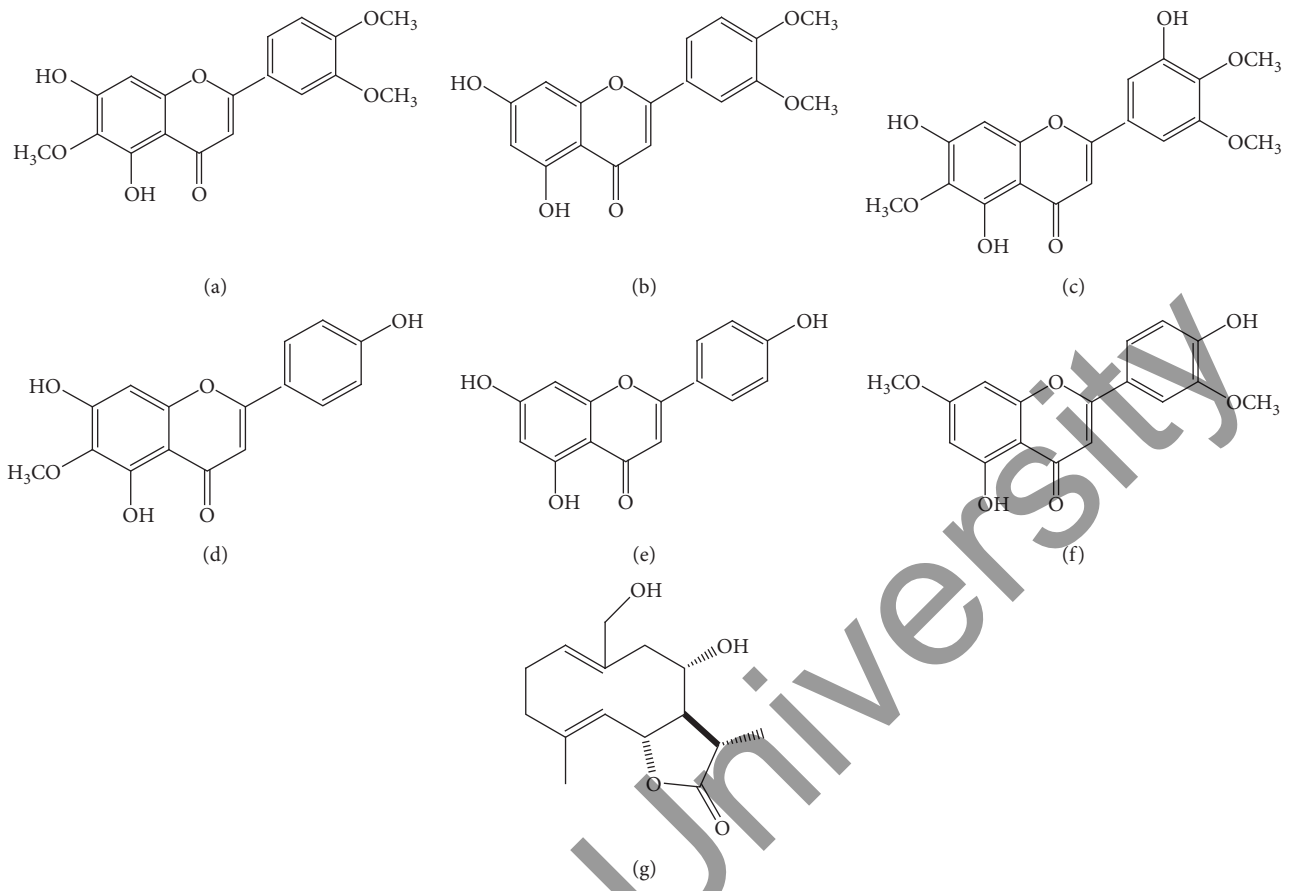

Figure 1: Chemical structures of the isolated compounds.

Table 1: The docking binding free energies of seven compounds, simeprevir, and the cocrystallized ligand (PRD-002214) against COVID-19 main protease.

Compound	Binding free energy (kcal/mol)
1	−6.53
2	−6.81
3	−6.51
4	−6.44
5	−6.39
6	−6.55
7	−4,94
Cocrystallized ligand (PRD-002214)	−7.83

The crystallized ligand (PRD-002214) showed binding energy of −7.83 kcal/mol. The detailed binding mode of the crystallized ligand was as follows: making three hydrogen bonds with Phe140, His163, and Glu166, the 2-oxopyrrolidin-3-yl moiety occupied the first pocket of the enzyme. Additionally, tert-butyl carbamate moiety occupied the second pocket of M^{pro}. Furthermore, the phenyl ring of phenylalanine moiety occupied the third pocket of the receptor, forming hydrophobic interaction with His41. Finally, ethyl propionate moiety was incorporated in the fourth pocket (Figures 2–4).

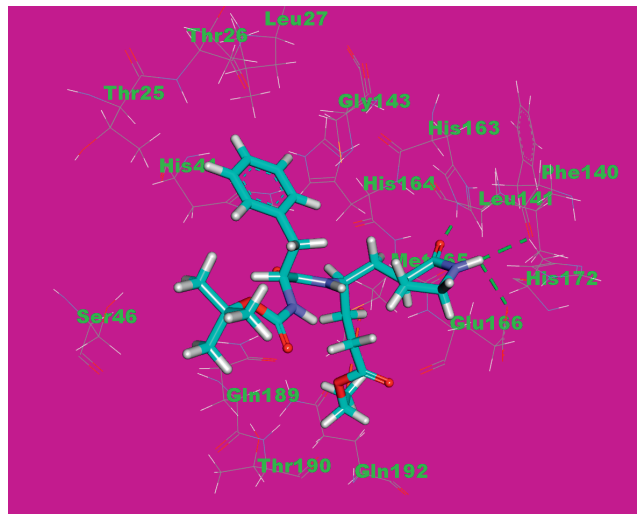

Figure 2: Cocrystallized ligand (PRD-002214) docked into the active site of the COVID-19 main protease. The hydrogen bonds are represented in green dashed lines, and the hydrophobic interactions are represented in orange dashed lines.

Compound (2) showed the best binding mode and highest binding energy of −6.81 kcal/mol. The 7-hydroxy-6-methoxy-4H-chromen-4-one moiety occupied the first pocket of M^{pro}, forming three hydrogen bonds with Phe140

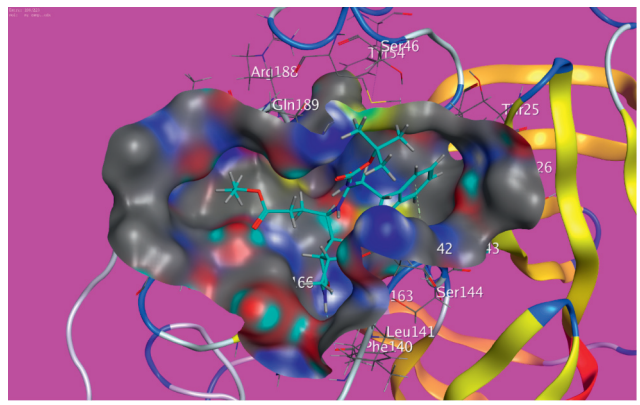

Figure 3: Mapping surface showing the cocrystallized ligand (PRD-002214) occupying the active pocket of the COVID-19 main protease.

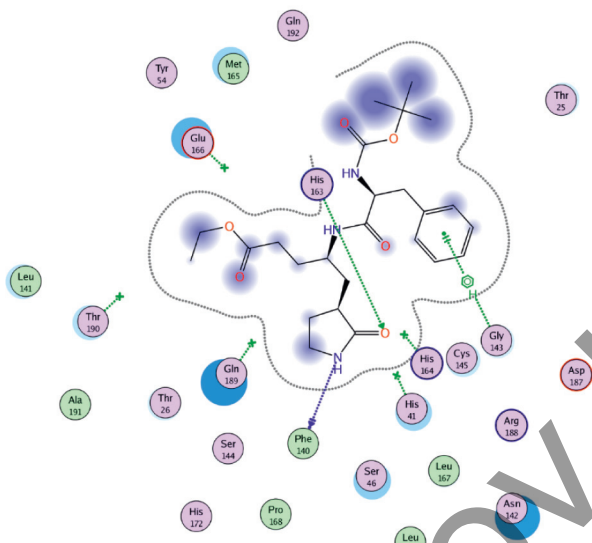

Figure 4: 2D interaction of the cocrystallized ligand (PRD-002214) in the active site of the COVID-19 main protease.

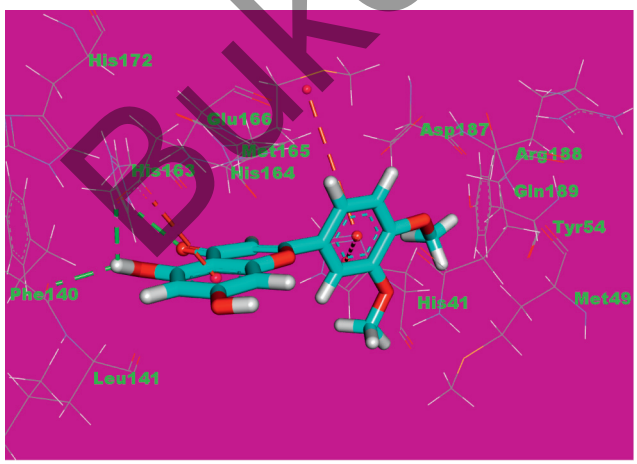

Figure 5: Compound (2) docked into the active site of the COVID-19 main protease. The hydrogen bonds are represented in green dashed lines, and the hydrophobic interactions are represented in orange dashed lines.

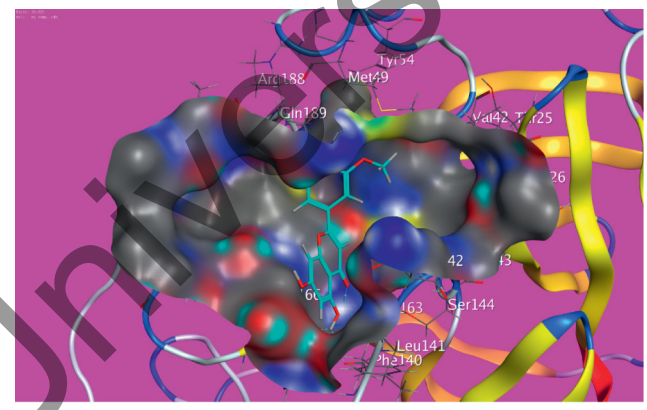

Figure 6: Mapping surface showing compound (2) occupying the active pocket of the COVID-19 main protease.

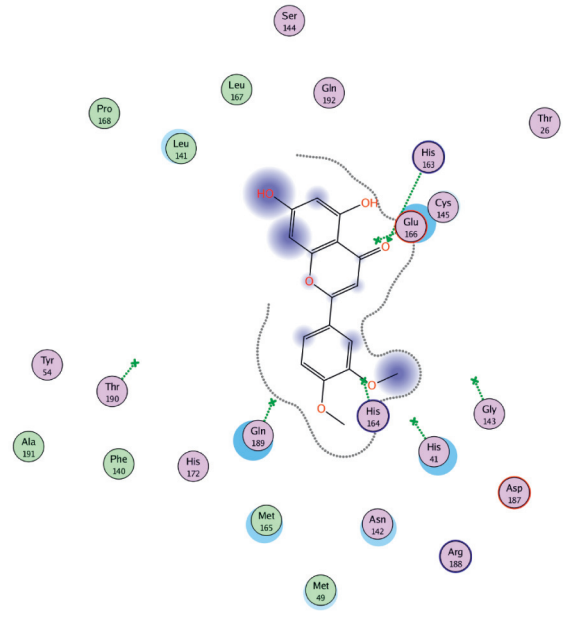

Figure 7: 2D interaction of compound (2) in the active site of the COVID-19 main protease.

and His163. Also, it formed one hydrophobic interaction with His163. Additionally, 1,2-dimethoxybenzene moiety occupied the second pocket of M^{pro} forming two hydrophobic interactions with Met165 and His41 (Figures 5–7).

4. Conclusions

This study focused on the phytochemical and the *in silico* biological investigation against the COVID-19 main protease (M^{pro}) of six flavonoids and one sesquiterpene lactone obtained from *A. sublessingiana*. Eupatilin, 3′, 4′-dimethoxyluteolin, 5, 7, 3′-trihydroxy-6, 4′,5′-trimethoxyflavone, velutin, and 8α,14-dihydroxy-11,13-dihydromelampolide were isolated from *Artemisia* species for the first time. Compound (2) exhibited the best binding mode with a binding energy of −6.81 kcal/mol against COVID-19 main protease (M^{pro}). The obtained results open a window of hope to find an effective cure to the pandemic of COVID-19. Further *in vitro* and clinical studies should be conducted on compound 2 to confirm its potential against the contagious virus SARS-CoV-2.

Data Availability

NMR data of the isolated compounds are available.

Conflicts of Interest

The authors declare that they have no conflicts of interest.

Acknowledgments

This work was supported by the Matsumae International Foundation grant (Japan) and has been funded by the Science Committee of the Ministry of Education and Science of the Republic of Kazakhstan (Grant no. AP 05130941).

Supplementary Materials

Supplementary materials contain the ^{1}H, ^{13}C, 2D NMR, and ESI-MS data for compounds 1–7. (*Supplementary Materials*)

References

[1] I. Steffens, "A hundred days into the coronavirus disease (COVID-19) pandemic," *Eurosurveillance*, vol. 25, Article ID 2000550, 2020.

[2] WHO, *WHO Coronavirus Disease (COVID-19) Dashboard*, WHO, Geneva, Switzerland, 2020, https://covid19.who.int/.

[3] G. Li and E. De Clercq, "Therapeutic options for the 2019 novel coronavirus (2019-nCoV)," *Nature Reviews Drug Discovery*, vol. 19, no. 3, pp. 149-150, 2020.

[4] N. Zhong, B. Zheng, Y. Li et al., "Epidemiology and cause of severe acute respiratory syndrome (SARS) in Guangdong, People's Republic of China, in February, 2003," *The Lancet*, vol. 362, no. 9393, pp. 1353–1358, 2003.

[5] R. J. de Groot, S. C. Baker, R. S. Baric et al., "Middle East respiratory syndrome coronavirus (MERS-CoV): announcement of the coronavirus study group," *Journal of Virology*, vol. 87, no. 14, pp. 7790–7792, 2013.

[6] W. Dai, B. Zhang, X.-M. Jiang et al., "Structure-based design of antiviral drug candidates targeting the SARS-CoV-2 main protease," *Science*, vol. 368, no. 6497, pp. 1331–1335, 2020.

[7] K. Anand, G. J. Palm, J. R. Mesters, S. G. Siddell, J. Ziebuhr, and R. Hilgenfeld, "Structure of coronavirus main proteinase reveals combination of a chymotrypsin fold with an extra alpha-helical domain," *The EMBO Journal*, vol. 21, pp. 3213–3224, 2002.

[8] H. Yang, M. Yang, Y. Ding et al., "The crystal structures of severe acute respiratory syndrome virus main protease and its complex with an inhibitor," *Proceedings of the National Academy of Sciences*, vol. 100, no. 23, pp. 13190–13195, 2003.

[9] R. Hilgenfeld, "From SARS to MERS: crystallographic studies on coronaviral proteases enable antiviral drug design," *FEBS Journal*, vol. 281, no. 18, pp. 4085–4096, 2014.

[10] L. Zhang, D. Lin, X. Sun et al., "Crystal structure of SARS-CoV-2 main protease provides a basis for design of improved α-ketoamide inhibitors," *Science*, vol. 368, no. 6489, pp. 409–412, 2020.

[11] M. A. A. Ibrahim, K. A. A. Abdeljawaad, A. H. M. Abdelrahman, and M.-E. F. Hegazy, "Natural-like products as potential SARS-CoV-2 Mpro inhibitors: in-silico drug discovery," *Journal of Biomolecular Structure and Dynamics*, vol. 7, pp. 1–13, 2020.

[12] M. A. A. Ibrahim, A. H. M. Abdelrahman, T. A. Hussien et al., "In silico drug discovery of major metabolites from spices as SARS-CoV-2 main protease inhibitors," *Computers in Biology and Medicine*, vol. 126, Article ID 104046, 2020.

[13] A. A. Al-Karmalawy and I. H. Eissa, "Molecular docking and dynamics simulations reveal the potential of anti-HCV drugs to inhibit COVID-19 main protease," *Pharmaceutical Sciences*, 2021.

[14] A. M. Metwaly, Z. Lianlian, H. Luqi, and D. Deqiang, "Black ginseng and its saponins: preparation, phytochemistry and pharmacological effects," *Molecules*, vol. 24, no. 10, p. 1856, 2019.

[15] Y.-M. Wang, X.-K. Ran, M. Riaz et al., "Chemical constituents of stems and leaves of *Tagetespatula* L. and its fingerprint," *Molecules*, vol. 24, no. 21, p. 3911, 2019.

[16] A. El-Demerdash, A. M. Metwaly, A. Hassan et al., "Comprehensive virtual screening of the antiviral potentialities of marine polycyclic guanidine alkaloids against SARS-CoV-2 (COVID-19)," *Biomolecules*, vol. 11, no. 3, p. 460, 2021.

[17] S. V. Sperstad, T. Haug, H.-M. Blencke, O. B. Styrvold, C. Li, and K. Stensvåg, "Antimicrobial peptides from marine invertebrates: challenges and perspectives in marine antimicrobial peptide discovery," *Biotechnology Advances*, vol. 29, no. 5, pp. 519–530, 2011.

[18] A. M. Metwaly, A. S. Wanas, M. M. Radwan, S. A. Ross, and M. A. ElSohly, "New α-Pyrone derivatives from the endophytic fungus *Embellisia* sp," *Medicinal Chemistry Research*, vol. 26, no. 8, pp. 1796–1800, 2017.

[19] A. Metwaly, H. Kadry, A. El-Hela, A. Elsalam, and S. Ross, "New antimalarial benzopyran derivatives from the endophytic fungus Alternaria phragmospora," *Planta Medica*, vol. 80, no. 10, p. PC11, 2014.

[20] A. Metwaly, "Comparative biological evaluation of four endophytic fungi isolated from *Nigella sativa* seeds," *Al-Azhar Journal of Pharmaceutical Sciences*, vol. 59, no. 1, pp. 123–136, 2019.

[21] M. H. Sharaf, G. M. El-Sherbiny, S. A. Moghannem et al., "New combination approaches to combat methicillin-resistant *Staphylococcus aureus* (MRSA)," *Scientific Reports*, vol. 11, pp. 1–16, 2021.

[22] A. M. Yassin, N. M. El-Deeb, A. M. Metwaly, G. F. El Fawal, M. M. Radwan, and E. E. Hafez, "Induction of apoptosis in human cancer cells through extrinsic and intrinsic pathways by *Balanites aegyptiaca* furostanol saponins and saponin-coated silver nanoparticles," *Applied Biochemistry and Biotechnology*, vol. 182, no. 4, pp. 1675–1693, 2017.

[23] A. Zhanzhaxina, Y. Suleimen, A. M. Metwaly et al., "*In vitro* and *in silico* cytotoxic and antibacterial activities of a diterpene from cousinia alata schrenk," *Journal of Chemistry*, vol. 2021, Article ID 5542455, , 2021.

[24] A. M. Metwaly, F. R. Fronczek, G. Ma et al., "Antileukemic α-pyrone derivatives from the endophytic fungus *Alternaria phragmospora*," *Tetrahedron Letters*, vol. 55, no. 24, pp. 3478–3481, 2014.

[25] A. M. Metwaly, H. A. Kadry, A. A. El-Hela et al., "Nigrosphaerin A a new isochromene derivative from the endophytic fungus *Nigrospora sphaerica*," *Phytochemistry Letters*, vol. 7, pp. 1–5, 2014.

[26] M. M. Ghoneim, W. M. Afifi, M. Ibrahim et al., "Biological evaluation and molecular docking study of metabolites from *Salvadora persica* L. growing in Egypt," *Pharmacognosy Magazine*, vol. 15, p. 232, 2019.

[27] L. Liu, S. Luo, M. Yu et al., "Chemical constituents ofTagetes patulaand their neuroprotecting action," *Natural Product Communications*, vol. 15, no. 11, 2020.

[28] A. M. Metwaly, M. M. Ghoneim, and A. Musa, "Two new antileishmanial diketopiperazine alkaloids from the endophytic fungus *Trichosporum* sp," *Derpharmachemica*, vol. 7, no. 11, pp. 322–327, 2015.

[29] N. F. Kane, M. C. Kyama, J. K. Nganga, A. Hassanali, M. Diallo, and F. T. Kimani, "Comparison of phytochemical profiles and antimalarial activities of *Artemisia afra* plant collected from five countries in Africa," *South African Journal of Botany*, vol. 125, pp. 126–133, 2019.

[30] V. Zarezade, J. Moludi, M. Mostafazadeh, M. Mohammadi, and A. Veisi, "Antioxidant and hepatoprotective effects of *Artemisia dracunculus* against CCl_4-induced hepatotoxicity in rats," *Avicenna Journal of Phytomedicine*, vol. 8, p. 51, 2018.

[31] S. Salehi, A. Mirzaie, S. A. Sadat Shandiz et al., "Chemical composition, antioxidant, antibacterial and cytotoxic effects of Artemisia marschalliana Sprengel extract," *Natural Product Research*, vol. 31, no. 4, pp. 469–472, 2017.

[32] T. Ruakhovskaya, A. Manadilova, and O. Sapco, *The Flavonoids of Artemisia-Sublessingiana. Akademiya Nauk Uzbekskoi ssr ul Kuibysheva 15*, p. 407, Tashkent, Uzbekistan, 1985.

[33] V. A. Tarasov, S. Z. Kasymov, and G. P. Sidyakin, "The structure of the *Sesquiterpene lactone* arsubin," *Chemistry of Natural Compounds*, vol. 7, no. 6, pp. 722-723, 1971.

[34] U. G. Ryahovskaya and F. G. Zhemaletdinov, "Antitumor activity of phenolic compounds from some Artemisia L. species," *Rastitel'nye Resursy*, vol. 25.

[35] H. Yuan, X. Lu, Q. Ma, D. Li, G. Xu, and G. Piao, "Flavonoids from Artemisia sacrorum Ledeb. and their cytotoxic activities against human cancer cell lines," *Experimental and Therapeutic Medicine*, vol. 12, no. 3, pp. 1873–1878, 2016.

[36] A. Galkina, N. Krause, M. Lenz, C. G. Daniliuc, M. Kaiser, and T. J. Schmidt, "Antitrypanosomal activity of sesquiterpene lactones from *Helianthus tuberosus* L. Including a new furanoheliangolide with an unusual structure," *Molecules*, vol. 24, no. 6, p. 1068, 2019.

[37] R. G. Kudumela, O. Mazimba, and P. Masoko, "Isolation and characterisation of *Sesquiterpene lactones* from *Schkuhria pinnata* and their antibacterial and anti-inflammatory activities," *South African Journal of Botany*, vol. 126, pp. 340–344, 2019.

[38] N. Martins, S. Petropoulos, and I. C. F. R. Ferreira, "Chemical composition and bioactive compounds of garlic (*Allium sativum* L.) as affected by pre- and post-harvest conditions: a review," *Food Chemistry*, vol. 211, pp. 41–50, 2016.

[39] K. M. El-Gamal, A. M. El-Morsy, A. M. Saad, I. H. Eissa, and M. Alswah, "Synthesis, docking, QSAR, ADMET and antimicrobial evaluation of new quinoline-3-carbonitrile derivatives as potential DNA-gyrase inhibitors," *Journal of Molecular Structure*, vol. 1166, pp. 15–33, 2018.

[40] M. K. Ibrahim, I. H. Eissa, M. S. Alesawy, A. M. Metwaly, M. M. Radwan, and M. A. ElSohly, "Design, synthesis, molecular modeling and anti-hyperglycemic evaluation of quinazolin-4(3H)-one derivatives as potential PPARγ and SUR agonists," *Bioorganic & Medicinal Chemistry*, vol. 25, no. 17, pp. 4723–4744, 2017.

[41] S. A. Elmetwally, K. F. Saied, I. H. Eissa, and E. B. Elkaeed, "Design, synthesis and anticancer evaluation of thieno[2, 3-d] pyrimidine derivatives as dual EGFR/HER2 inhibitors and apoptosis inducers," *Bioorganic Chemistry*, vol. 88, Article ID 102944, 2019.

[42] H. A. Mahdy, M. K. Ibrahim, A. M. Metwaly et al., "Design, synthesis, molecular modeling, in vivo studies and anticancer evaluation of quinazolin-4(3H)-one derivatives as potential VEGFR-2 inhibitors and apoptosis inducers," *Bioorganic Chemistry*, vol. 94, Article ID 103422, 2020.

[43] M. A. El-Zahabi, E. R. Elbendary, F. H. Bamanie, M. F. Radwan, S. A. Ghareib, and I. H. Eissa, "Design, synthesis, molecular modeling and anti-hyperglycemic evaluation of phthalimide-sulfonylurea hybrids as PPARγ and SUR agonists," *Bioorganic Chemistry*, vol. 91, Article ID 103115, 2019.

[44] S. M. Kupchan, C. W. Sigel, R. J. Hemingway, J. R. Knox, and M. S. Udayamurthy, "Tumor inhibitors-XXXIII," *Tetrahedron*, vol. 25, no. 8, pp. 1603–1615, 1969.

[45] Y.-R. Deng, A.-X. Song, and H.-Q. Wang, "Chemical components of *Seriphidium Santolium* Poljak," *Journal of the Chinese Chemical Society*, vol. 51, no. 3, pp. 629–636, 2004.

[46] T. Nakanishi, J. Ogaki, A. Inada et al., "Flavonoids of *Striga asiatica*," *Journal of Natural Products*, vol. 48, no. 3, pp. 491–493, 1985.

[47] F. Dal Piaz, A. Bader, N. Malafronte et al., "Phytochemistry of compounds isolated from the leaf-surface extract of *Psiadia punctulata* (DC.) Vatke growing in Saudi Arabia," *Phytochemistry*, vol. 155, pp. 191–202, 2018.

[48] H. Gao and J. Kawabata, "Importance of the B ring and its substitution on the α-glucosidase inhibitory activity of baicalein, 5,6,7-Trihydroxyflavone," *Bioscience, Biotechnology, and Biochemistry*, vol. 68, no. 9, pp. 1858–1864, 2004.

[49] Р. Р. Фаильевна, Чимия растительноҐо сырья, pp. 233–236, 2017.

[50] Y.-L. Liu, D. K. Ho, J. M. Cassady, V. M. Cook, and W. M. Baird, "Isolation of potential cancer chemopreventive agents from *Eriodictyon californicum*," *Journal of Natural Products*, vol. 55, no. 3, pp. 357–363, 1992.

[51] W. Herz and Y. Sumi, "Constituents of *Ambrosia hispida* Pursh.1,2," *The Journal of Organic Chemistry*, vol. 29, no. 11, pp. 3438-3439, 1964.

[52] T. Ryakhovskaya, O. Sapko, A. Manadilova, G. Ushhaeva, and S. Bokaeva, "Polyphenols of sagebrush and biological activity of its phenolic complex–FECS," in *Proceedings of the International Conference on Plant Synthetic Biology, Bioengineering, and Biotechnology*, Beijing, China, 1987.

[53] Y. Teles, C. Horta, M. Agra et al., "New sulphated flavonoids from *Wissadula periplocifolia* (L.) C. Presl (*Malvaceae*)," *Molecules*, vol. 20, no. 11, pp. 20161–20172, 2015.

[54] H. Sayed, M. Mohamed, S. Farag et al., "Phenolics of *Cyperus alopecuroides* rottb. Inflorescences and their biological activities," *Bulletin of Pharmaceutical Sciences. Assiut*, vol. 29, no. 1, pp. 9–32, 2006.

[55] P. Singh, A. K. Sharma, K. C. Joshi, J. Jakupovic, and F. Bohlmann, "Acanthospermolides and other constituents from *Blainvillea acmella*," *Phytochemistry*, vol. 24, no. 9, pp. 2023–2028, 1985.

[56] A. Rustaiyan, K. Zare, M. T. Ganj, and H. A. Sadri, "A melampolide and two dihydro artemorin derivatives from *Artemisia gypsacea*," *Phytochemistry*, vol. 28, no. 5, pp. 1535-1536, 1989.

[57] J. F. Sanz, A. Rustaiyan, and J. A. Marco, "A melampolide from *Artemisia oliveriana*," *Phytochemistry*, vol. 29, no. 9, pp. 2919–2921, 1990.